Characterization of Cross-Linked Rubber Materials via Proton Rotating-Frame Relaxation Measurements

H. Chaumette, D. Grandclaude, P. Tekely, and D. Canet*

Laboratoire de Méthodologie RMN†, Université H. Poincaré, Nancy I, BP 239, 54506 Vandoeuvre-lès-Nancy (Cedex), France

C. Cardinet and A. Verschave

Hutchinson S.A., Centre de Recherche, Rue Gustave Nourry, BP 31, 45120 Châlette-sur-Loing, France

Received: January 10, 2001; In Final Form: July 6, 2001

Proton relaxation times in the rotating frame, as obtained from the decay of nuclear magnetization locked along a radio frequency field B_1, have been measured in a series of cross-linked natural rubber materials. These decays are monoexponential and the relevant time constants, $T_{1\rho}$, can be monitored as a function of the radio frequency field strength B_1. At any B_1 value, they appear to be correlated in a very sensitive way to the cross-link density. A novel interpretation of the $T_{1\rho}$ dependence upon B_1 is presented. It is based on a theory describing the evolution of a two spin 1/2 system coupled by dipolar interaction in the presence of a spin-locking field. The measured rotating-frame relaxation rate is shown to be equal to the sum of the motionally related $1/T_{1\rho}$ and a term arising from the radio frequency field inhomogeneity. Both terms are proportional to the square of the dipolar interaction (the second moment in the present case where a distribution of dipolar interactions exists). Concerning changes of cross-link density, $T_{1\rho}$ measurements provide therefore a more direct information than transverse relaxation measurements (also performed in this study), the composite nature of the latter decay curves making their interpretation less straightforward. As a complement to the present relaxation study, we show the correlation of the self-diffusion coefficient of a solvent imbedded in the material with rubber $T_{1\rho}$ values.

Introduction

Nuclear magnetic resonance (NMR) plays an important role in the study of cross-linked elastomers. The relevant techniques include nuclear spin relaxation time determinations,[1−10] NMR microscopy,[11−15] and solid-state ^{13}C NMR.[16−24] Solid-state methods are usually invoked for determining residual dipolar couplings which are directly related to polymer dynamic properties[25] and proton relaxation times may constitute the basis of contrast in imaging experiments. Basically, three relaxation times can be invoked: the spin−lattice or longitudinal relaxation time, T_1, the spin−spin or transverse relaxation time, T_2, and the rotating-frame relaxation time $T_{1\rho}$. The longitudinal relaxation time is of limited interest at high measuring frequencies (100 MHz or more) because it probes fast motions which are not very specific of the chemical structure of polymer chains. Clearly, for being useful, it should be measured at low frequencies (below 10 MHz), in a range relevant to the so-called relaxometry techniques.[26] This poses the problem of extensive measurements which make the method difficult to apply on a routine basis. Transverse relaxation is appealing as it is in principle sensitive to slow motions and thus capable of providing information about motional constrains from cross-links and entanglements. However, the decay of transverse magnetization may be somewhat complicated as it invokes first a Gaussian decay related to residual dipolar couplings and thereafter one (or more) exponential decay(s) related to effective spin−spin relaxation time(s).[4] Surprisingly, the rotating-frame relaxation time (measured by spin-locking the nuclear magnetization along the radio frequency field) has received little attention in the study of rubber materials, although its experimental determination and its spectroscopic response are much more simple. In fact, to the best of our knowledge, proton longitudinal relaxation in the rotating frame has been so far exploited in cross-linked polymers only to study the interaction between carbon black and elastomers[27,28] and as a tool in relaxation weighted imaging.[13]

In this work, we will demonstrate the usefulness of this relaxation parameter for monitoring the changes of the relative cross-link density (within a given series of samples). It will be indeed shown that $T_{1\rho}$ at a given radio frequency field strength represents a sort of fingerprint of cross-link density, presumably more reliable than the traditional M_C, the inter-*cross*-link chain mass usually determined by solvent penetration.[29] Moreover, the evolution of the measured $T_{1\rho}$ versus the radio frequency field strength has been consistently analyzed and shown to provide two parameters directly related to the cross-link density: the true (motionally determined) $T_{1\rho}$ and an experimental factor describing the dependence with respect to the radio frequency field strength.

We will also present the measurements of the molecular self-diffusion coefficient of a solvent (toluene) within the corresponding rubber materials and will show that they are consistent with the $T_{1\rho}$ determination.

Experimental Section

We shall limit ourselves to a series of five samples of natural rubber prepared with different amounts of accelerator (CBS:

* Corresponding author.
† UPRESA CNRS 7042, INCM-FR CNRS 1742.

10.1021/jp010140a CCC: $20.00
Published on Web 09/06/2001

TABLE 1: Characteristics of the Investigated Rubber Samples, along with Pertinent Parameters Extracted from Transverse and Rotating-Frame Relaxation Experiments

sample	sulfur (phr)	black carbon (phr)	M_c	qM_2 (10^4 s^{-2})	R_2^s (s^{-1})	R_2^f (s^{-1})	$\bar{R}_2$ (s^{-1})	$R_{1\rho}^{\infty} \equiv k_0$ (s^{-1}; eq 3)	k_1 (eq 3)
G				4.8	205	50.2	183	37.7	98.9
A	1		11000	10.0	203	55.7	193	52.4	142.0
A_{cb}	1	40		8.2	200		205	48.5	118.9
B	2		6500	16.0	172	50.1	167	59.2	163.8
C	3		4600	13.8	174	50.9	177	75.4	185.7
D	4		4000	32.4	233	62.4	186	103.2	277.0
E	5		3100	18.1	255	64.9	217	121.5	377.0
E_{cb}	5	40		22.8	242		235	105.2	307.4

N-cyclohexylbenzothiazole-2-sulfenamide) and sulfur in such a way that the ratio sulfur/CBS is kept constant and equal to 1. Samples denoted by A to E correspond to increasing amount of sulfur and CBS from 1 to 5 phr. Also, a carbon black amount of 40 phr has been added to two samples, A and E, leading to materials denoted in the following by A_{cb} and E_{cb}. M_c was determined by the classical weight method by using the swelling process. For the sake of completeness, un-cross-linked natural rubber (sample G) was investigated only via its relaxation times as it cannot accommodate toluene uptake. Sample compositions are given in Table 1.

All NMR experiments have been carried out at 25 °C with a homemade spectrometer operating at 200 MHz. Decays of transverse magnetization (T_2 type experiments) were monitored according to the CPMG (Carr-Purcell-Meiboom-Gill) method.[30] The pulse sequence is as follows: $(\pi/2)_x$-τ-$[(\pi)_y$-τ-(Acq)-$\tau]_n$ in which ***x*** and ***y*** refer to the radio frequency (rf) phase while magnetization rotation angles are indicated between parentheses. The initial $(\pi/2)_x$ places the nuclear magnetization into the transverse plane where it is allowed to precess with refocusing midway consecutive $(\pi)_y$ pulses (spin−echo formation). The echo amplitude is measured thus sampling the decay of transverse magnetization independently of precession phenomena including those associated with the main magnetic field inhomogeneity. Thanks to extensive rf phase changes, imperfections of π pulses are compensated for at every even echo and, in fact, signal acquisition is limited to these even echoes. Another advantage of the CPMG method is that the decay of transverse magnetization is obtained in a single experiment, i.e., in a one-shot manner. Nevertheless, several experiments have been performed with different intervals, 2τ, between two consecutive π pulses: 100 μs,120 μs, 140 μs, 160 μs. They did not exhibit any significant change.

Relaxation times in the rotating frame ($T_{1\rho}$) have been measured through the classical pulse sequence[30] $(\pi/2)_x$(SL)$_y$-(Acq) where ***x*** and ***y*** denote again the radio frequency phase, while (SL) stands for a spin lock period whose length is varied typically between 1 ms and 30 ms. This decay of magnetization locked along the rf field direction was measured from the peak integral intensity changes and, in all cases, it proved to be perfectly monoexponential yielding a well-defined time constant $T_{1\rho}$. As $T_{1\rho}$ depends on the rf field strength B_1, several experiments have been performed with $\gamma B_1/2\pi$ (γ: gyromagnetic ratio) varying between 10 kHz (below this value, which is slightly greater than the proton line-width, measurements would presumably be meaningless) and 110 kHz. The latter value represents a fairly high rf field requiring a special homemade probe equipped with tuning and matching capacitors capable of standing high rf power (Polyflon RPVC 10-12). The probe is designed for 5 mm o.d. NMR tubes and needs a transmitter output power of 210 W for $(\gamma B_1/2\pi) = 110$ kHz, corresponding to a $(\pi/2)$ pulse duration of 2.3 μs.

For studying the self-diffusion of toluene, two series of samples were prepared. One corresponds to maximum (or total) swelling requiring an immersion time of several days; the other corresponds to a partial swelling obtained after an immersion of 30 min. The samples were pulled out from the solvent container, wiped, and placed in the NMR sample tube which was immediately sealed. Self-diffusion coefficients, D, were measured with a method based on rf field gradients developed in this laboratory.[31] It is especially well adapted to heterogeneous samples and relies on the decay of longitudinal magnetization evolving in the presence of two identical rf field gradient pulses separated by an interval called the diffusion interval. The first gradient pulse defocuses by spatially dependent nutation the magnetization initially aligned with the static magnetic field B_0; complete refocusing by the second gradient pulse would occur in the absence of translational diffusion. This is because the defocusing−refocusing process originates from spatial labeling; complete refocusing requires that molecules bearing nuclear spins see the same rf field during the application of the two gradient pulses, otherwise the refocusing is incomplete and depends on molecular diffusion according to a well-known law[30] yielding the self-diffusion coefficient. All measurements were performed with a rf field gradient of 30 G/cm and a diffusion interval of 400 ms, the value of the self-diffusion coefficient was deduced from the variation of the integral intensity of the proton signals of toluene subjected to gradient pulses whose duration ranges from 100 μs to 1 ms.

Results and Interpretation

Transverse Relaxation. The proton NMR spectra for all samples under study are broad, structureless and of complex shape.[20] Some typical spectra are shown in Figure 1. They contain the inhomogeneous broadening which represents the "solidlike" contribution related to the static nonzero average value of the dipolar Hamiltonian. This contribution to the line-width leads to a coherent, or reversible time evolution, which can be refocused by appropriate pulse sequences.[24] The remaining part of the line width comes from the homogeneous broadening due to relaxation effects arising from rapid fluctuations of the dipolar Hamiltonian. A deeper insight into the basic characteristics of the proton system is available by resorting to the CPMG experiment. In fact, the examination of the transverse relaxation decay curves shown in Figure 2 enables one to visualize the existence of two regimes. The initial decay is approximately Gaussian-like and is due to dipolar interactions of protons in chain segments, averaged by the fast anisotropic local motion like a single bond rotation and counter-rotation between isomeric transition states. The anisotropy of this chain motion results from chemical cross-links and entanglements and leads to small residual dipolar couplings which may be treated by statistical chain models.[6] The second regime of the curve involves *two* exponential decays related to pure transverse

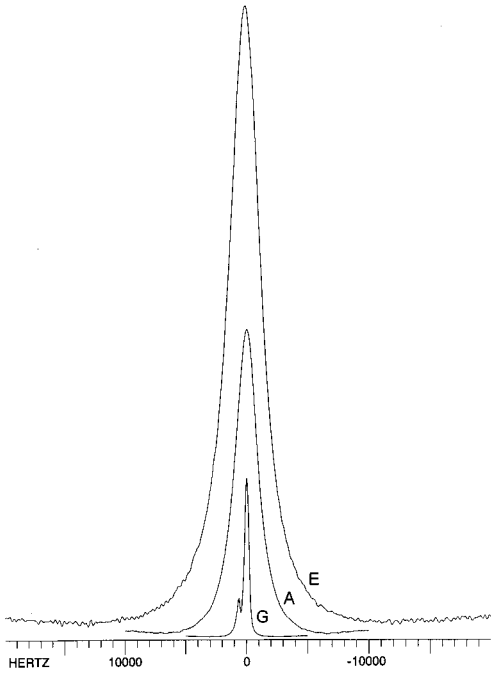

Figure 1. Proton spectra of samples G (natural rubber), A (least cross-linked in the series), and E (most cross-linked in the series). Note the small low-field peak in sample G due to olefinic protons (visible here thanks to smaller line widths).

relaxation processes. Its first stage is due to the rapid motions of free chain ends and of low molecular mass un-cross-linked chains originally present in natural rubber. This motion is assumed to be largely dominated by the rapid local reorientations having the same correlation times as the local motion of inter cross-link chain segments. The end of the decay curve, hardly visible for some samples, due to the smallness of the NMR signal at these long times, is most probably due to sol molecules or admixtures of high mobility which indeed may be eliminated or reduced by an extraction procedure.[4] The decay of transverse magnetization *S(t)* can thus be described according to a function successfully exploited earlier in rubber materials.[4] Taking into account the liquidlike contribution, this function in its simplest form takes the form

$$S(t) = a\exp(-R_2^f t - qM_2 t^2/2) + b\exp(-R_2^f t) + c\exp(-R_2^l t) \quad (1)$$

where ***a***, ***b***, and ***c*** are the amplitudes of the three stages (these quantities are necessary for fitting the experimental data; as their interpretation is rather difficult they will not be considered further); R_2^f and R_2^l are the transverse relaxation rates associated with fast local motion of inter and outer cross-link segments and liquidlike motions of sol molecules, respectively; qM_2 is a fraction of the second moment and will be simply considered here as an indication of the residual dipolar interaction strength; its trend is, as expected, to increase with the cross-link density although its accuracy is questionable (due to the fact that the nature of the CPMG experiment prevents a proper determination of the beginning of the decay curve) and does not make it a reliable parameter. The three parameters (qM_2, R_2^f, and R_2^l) are given in Table 1. Because R_2^f and R_2^l are not determined very accurately, an effective transverse relaxation rate, $\bar{R}_2$, obtained from the average decay of the nonGaussian part is also provided in Table 1. It can be noticed that no obvious tendency appears, this parameter lying always around 200 s^{-1}. It can also be stressed that entanglements may influence this result because measurements have not been performed 120 °C above the glass transition temperature (here $T_g \approx -70$ °C).

Rotating-Frame Relaxation Times. Experimental results, in terms of $R_{1\rho}$ (denoted below as $R_{1\rho}(\nu_1)$ or $R_{1\rho}^{app}$) which is the inverse of the rotating-frame relaxation time, are shown in Figure 3. A remarkable feature is the hierarchy of these curves which is related to the cross-link density and thus to residual dipolar couplings. Another striking feature is the observed dependence with respect to the spin-lock field amplitude expressed in Hz according to $\nu_1 = \gamma B_1/2\pi$. It is well-known[30] that, for systems involving slow motions, the rotating-frame relaxation rate, at a frequency ν_1, is dominated by a spectral density whose simplest form is $k\tau_c/(1 + 16\pi^2\nu_1^2\tau_c^2)$, k being a scaling factor and τ_c a correlation time associated with the relevant slow motion(s). In fact, it has been found that the experimental data could be successfully interpreted (standard deviation: s^{-1}) according to the expression given below:

$$R_{1\rho}(\nu_1) = k_0 + \frac{k_1\tau_c}{1 + 16\pi^2\nu_1^2\tau_c^2} \quad (2)$$

For all samples, a correlation time lying in the range 1.5−2 μs was obtained. Unfortunately, such a result is not in agreement with the correlation time derived from the $R_{1\rho}$ values at large ν_1 (see below). Moreover, for additional measurements that have been performed at ν_1 values below 10 kHz (not shown), a significant deviation occurs for the model given by eq 2 and this constitutes a further reason for discarding this model.

Although other spectral density functions can be invoked,[10,13] we have found that all experimental data could be accounted for by the following simple functional form:

$$R_{1\rho}(\nu_1) = k_0 + \frac{k_1}{\nu_1^\alpha} \quad (3)$$

Equation 3 can actually be justified by a theory consisting essentially of the derivation of eqs 4 and that will be presented in detail elsewhere. We shall just provide below an outline adapted to the present situation.

Let us consider a system of two spins 1/2, I and S, of identical chemical shift and coupled by a dipolar interaction ν_d (expressed in Hz). Their magnetizations are supposed to be spin-locked along the x axis by means of a rf field, the amplitude of which is denoted by ν_1 (see above). $\langle I_x + S_x\rangle$ is the quantity of interest, measured as a function of the duration of the spin-lock period. Due to the form of the dipolar Hamiltonian, it turns out that $\langle I_x + S_x\rangle$ is coupled to another quantity expressed as $\langle 2I_yS_z + 2I_zS_y\rangle$. The evolution equation of this latter quantity involves a third quantity $\langle 2I_yS_y - 2I_zS_z\rangle$. Altogether, the complete evolution of the spin system is governed by three simultaneous first-order differential equations:

$$\frac{d}{dt}\langle I_x + S_x\rangle = -R_{1\rho}\langle I_x + S_x\rangle - 2\pi\nu_d\langle 2I_yS_z + 2I_zS_y\rangle$$

$$\frac{d}{dt}\langle 2I_yS_z + 2I_zS_y\rangle = -R'_{1\rho}\langle 2I_yS_z + 2I_zS_y\rangle + 2\pi\nu_d\langle I_x + S_x\rangle + 2\pi\nu_1\langle 2I_yS_y - 2I_zS_z\rangle \quad (4)$$

$$\frac{d}{dt}\langle 2I_yS_y - 2I_zS_z\rangle = -R''_{1\rho}\langle 2I_yS_y - 2I_zS_z\rangle - 2\pi\nu_1\langle 2I_yS_z + 2I_zS_y\rangle$$

where $R_{1\rho}$, $R'_{1\rho}$ and $R''_{1\rho}$ are the specific rotating-frame relaxation rates of these three quantities. Although it is possible to

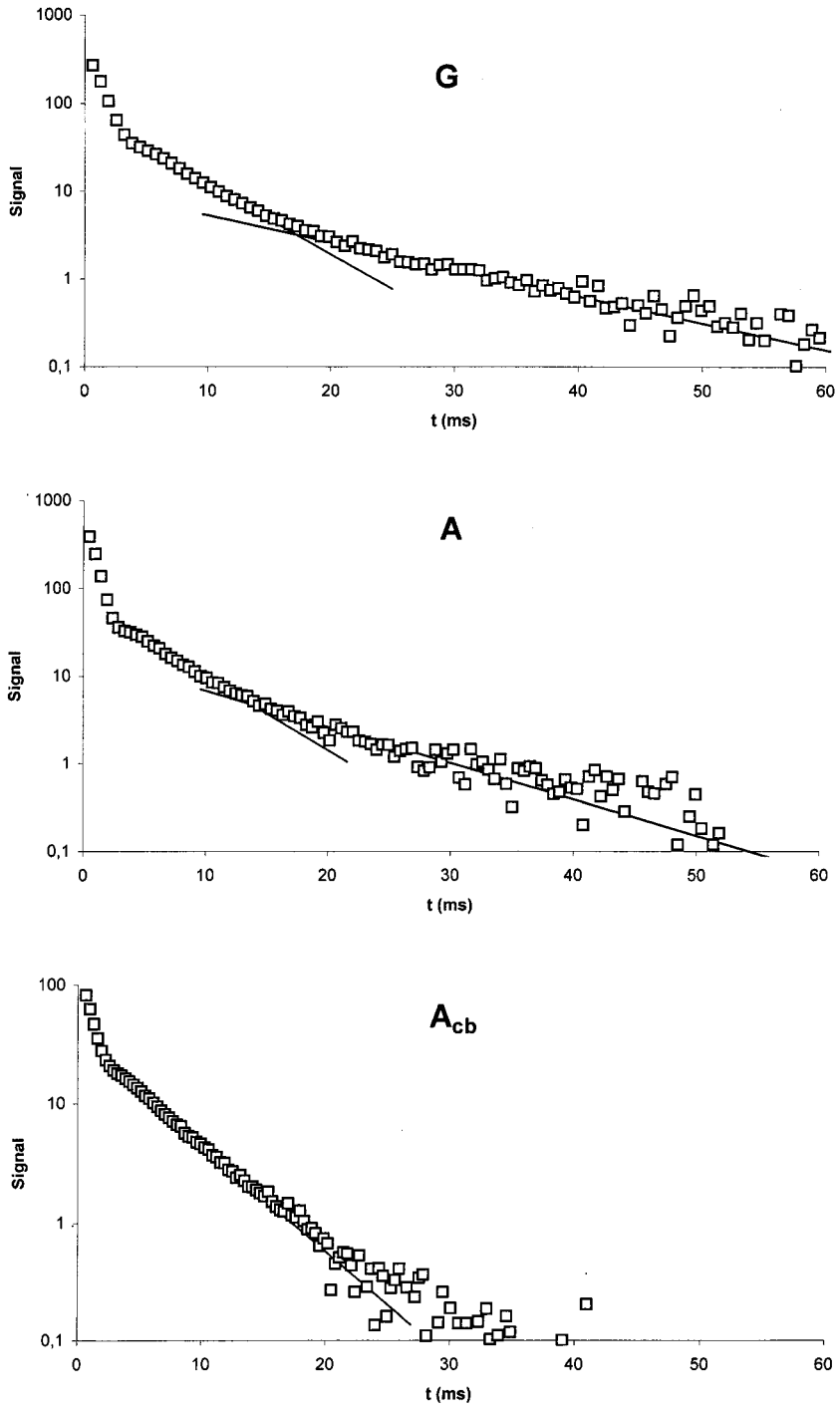

Figure 2. Experimental decays (squares) of transverse magnetization, measured by the CPMG method and presented as semilogarithmic plots for three representative samples: G (natural rubber), A (least cross-linked in the series), and A_{BC} (A with carbon black). The straight lines are associated with the two transverse relaxation rates R_2^f and R_2^l (see text and eq 1).

obtain an exact solution to these equations, we shall provide a simplified treatment based on assumptions appropriate to the present situation. First, we assume that the amplitude of the rf field is large enough so that ν_1 is the dominant term in the last two equations. Thus, with $u = \langle 2I_yS_z + 2I_zS_y\rangle$ we can write

$$u(t) = u(0)\cos(2\pi\nu_1 t) \qquad (5)$$

$u(0)$ being created from $\langle I_x + S_x\rangle$ through the coupling term with $\langle 2I_yS_z + 2I_zS_y\rangle$.

This tells us that u is subjected to nutation (or precession) under the rf field B_1 in a way similar to the familiar precession of nuclear magnetization under the static field B_0. In that latter case, it is well-known that precession is damped due to B_0 inhomogeneity leading to an effective transverse relaxation time T_2^* much shorter than the true T_2. As the rf field B_1 is also inhomogeneous, the evolution of $u = \langle 2I_yS_z + 2I_zS_y\rangle$ is dominated by an effective relaxation rate $R_{1\rho}^*$ much larger than $R_{1\rho}'$. Actually, the B_1 inhomogeneity increases with B_1 amplitude in a somewhat complicated manner, depending on the coil geometry, the sample filling factor, etc., so that we shall postulate that $R_{1\rho}^*$ is proportional to ν_1^α, where α is unknown (instrumental) parameter to be determined from the experimental data. Now, the coupling of $\langle 2I_yS_z + 2I_zS_y\rangle$ with $\langle 2I_yS_y - 2I_zS_z\rangle$ can be replaced by introducing $R_{1\rho}^*$ in the second equation of

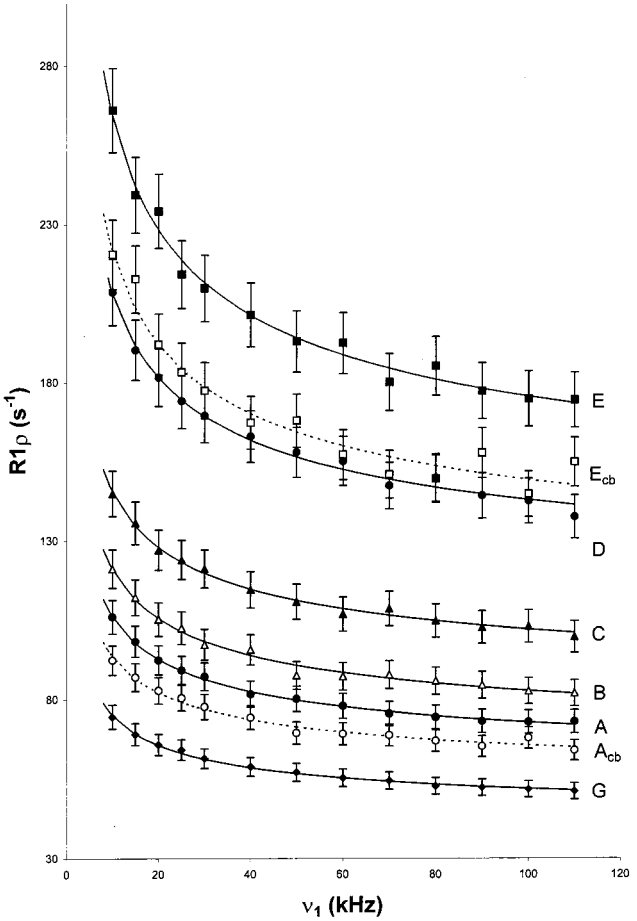

Figure 3. Results of the rotating-frame relaxation measurements as a function of the rf field amplitude B_1 (expressed as $\nu_1 = \gamma B_1/2\pi$). Continuous curves have been recalculated with parameters resulting from a fit according to eq 3.

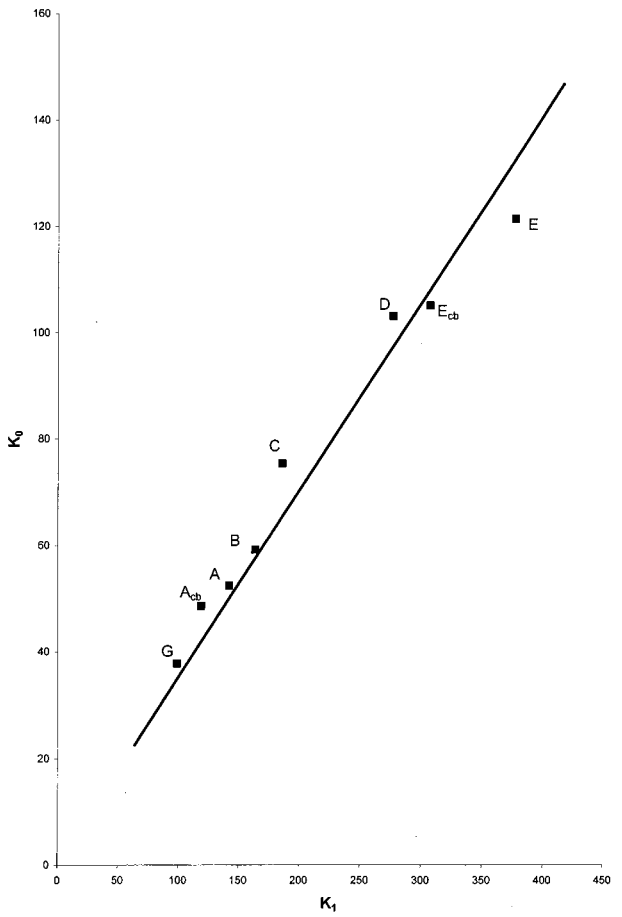

Figure 4. Plot showing the correlation between the two parameters, k_0 and k_1, involved in the interpretation of rotating-frame relaxation measurements (see eq 3).

eqs 4. This set of equations then reduces to

$$\frac{\mathrm{d}}{\mathrm{d}t}\langle I_x + S_x\rangle = -R_{1\rho}\langle I_x + S_x\rangle - 2\pi\nu_d\langle 2I_yS_z + 2I_zS_y\rangle$$

$$\frac{\mathrm{d}}{\mathrm{d}t}\langle 2I_yS_z + 2I_zS_y\rangle = -R^*_{1\rho}\langle 2I_yS_z + 2I_zS_y\rangle + 2\pi\nu_d\langle I_x + S_x\rangle \quad (6)$$

Denoting by $X = \langle I_x + S_x\rangle$ the quantity of interest (effectively measured), we obtain from eq 6

$$\frac{\mathrm{d}^2X}{\mathrm{d}t^2} + R^*_{1\rho}\frac{\mathrm{d}X}{\mathrm{d}t} + (R^*_{1\rho}R_{1\rho} + 4\pi^2\nu_d^2)X = 0 \quad (7)$$

where it has been assumed that $R^*_{1\rho} \gg R_{1\rho}$, as can be deduced from the characteristics of the usual NMR probes (in terms of rf field inhomogeneity) and from the known order of magnitude of $R_{1\rho}$.

For large values of the rf field amplitude, the rf field inhomogeneity and consequently $R^*_{1\rho}$ are large, too. In this limiting case of strong rf field, eq 7 reduces to

$$R^*_{1\rho}\frac{\mathrm{d}X}{\mathrm{d}t} + R^*_{1\rho}R_{1\rho}x = 0$$

thus

$$\frac{\mathrm{d}X}{\mathrm{d}t} + R_{1\rho}X = 0 \quad (8)$$

which leads to the familiar exponential evolution of the spin-locked magnetization according to the true rotating-frame relaxation rate $R_{1\rho}$. It can be noticed that, although eq 8 has been obtained through some approximations and assumptions related to the rf field strength and inhomogeneity, eq 8 would also have been derived from the whole set of eqs 4 by assuming that ν_1 is much greater than any other coefficient, independently of any B_1 inhomogeneity.

In the general case, eq 7 implies a biexponential solution. However, if we make again the realistic assumption that $R^*_{1\rho} \gg R_{1\rho}$, the actually observed part of the decay corresponds to the smallest root of the characteristic equation associated with eq 7, yielding an apparent rotating-frame relaxation rate of the form

$$R^{app}_{1\rho} = R_{1\rho} + \frac{4\pi^2\nu_d^2}{R^*_{1\rho}} \quad (9)$$

Remembering that $R^*_{1\rho}$ is proportional to ν_1^α, we can compare eq 9 and eq 3 and come to the conclusion that k_0 is just the $R_{1\rho}$ (which can thus be denoted as $R^\infty_{1\rho}$), whereas k_1 is proportional to ν_d^2. In fact, in our case we must consider the distribution of the residual dipolar couplings and consequently the average $\langle\nu_d^2\rangle$ which is nothing else than the second moment. As $R_{1\rho}$ should be proportional to the difference between the rigid lattice second moment (independent of cross-link density) and $\langle\nu_d^2\rangle$, there must exist a linear relationship between k_0 and k_1.

As samples have been prepared in an identical way, the exponent α should be the same for the whole set of experimental data which have therefore been fitted to a single value of α (a

TABLE 2: Self-diffusion Coefficients (10^{-5} cm^2 s^{-1}) of Toluene Inside the Rubber Sample for Different Immersion Times

sample	infinite immersion time	30 min immersion time
A	1.74	1.55
A_{cb}	1.40	1.00
B	1.60	1.40
C	1.51	1.30
D	1.25	1.00
E	1.17	0.95
E_{cb}	0.86	0.78

value of 0.42 was found) and to k_0 and k_1 for each sample. Recalculated curves, in excellent agreement with experimental data, are shown in Figure 3 whereas the values of k_0 and k_1 are given in Table 1. The hierarchy as a function of cross-link density (in other words, as a function of residual dipolar couplings) is perfectly respected and a linear relationship between k_0 and k_1 is indeed found (Figure 4) as predicted by the above theoretical considerations. It can be noticed that the adjunction of carbon black leads, as expected, to an apparent decrease of the cross-link density.

Finally, we can estimate a correlation time from the $R_{1\rho}^{\infty}$ values. Assuming that the correlation function associated with molecular motions is an exponential with a time constant τ_c (correlation time), it can be shown that the rotating-frame relaxation rate would depend on the spin-lock rf amplitude as[32]

$$R_{1\rho} = \Delta M_2 \tau_c \frac{1}{1 + 16\pi^2 \nu_1^2 \tau_c^2} \qquad (10)$$

where ΔM_2 is the difference between the rigid lattice second moment and the motionally averaged residual second moment. For natural rubber, ΔM_2 is approximately[13] 1.25×10^{10} s^{-2}. From eq 10 we can write

$$R_{1\rho}^{\infty} \cong \Delta M_2 \tau_c \qquad (11)$$

In our case, this lead to a τ_c value of $10^{-8}-10^{-9}$s, which is in good agreement with literature data relaxation concerning natural rubber.[33]

Toluene Self-Diffusion Coefficients. Since M_c is usually determined from the swelling properties of the considered material, it can be inferred that some other property related to solvent penetration would yield useful information regarding cross-link density. In this respect, translational diffusion of the solvent should be a good tool as it should be more hindered as the cross-link density increases. As indicated by the experimental results given in Table 2, this feature is actually verified regardless of the immersion time of the rubber sample in the considered solvent (here toluene). The evolution of the self-diffusion coefficients are indeed similar for a short immersion time (half an hour) and for a saturation state although, in the latter case, the effects are enhanced. As shown in Figure 5, the self-diffusion coefficient varies linearly with $T_{1\rho}$ which, as proved above, constitutes itself a very good indicator of cross-link density. Moreover, the observed shift corresponding to samples with black carbon visualizes well the fact that adjunction of black carbon decreases the relative quantity of polymer thus decreasing swelling concomitantly. As a consequence, solvent diffusion is more hindered leading to smaller self-diffusion coefficients.

Conclusion

Among the dynamic parameters which can be determined by NMR techniques, it appears that the rotating-frame relaxation time $T_{1\rho}$ yields, in a very sensitive way, an unambiguous information about changes of the relative cross-link density for a given series of rubber samples. Such a structural information can be easily achieved with measurements performed at a single value of the spin-lock radio frequency field amplitude. Furthermore, we have shown that the analysis of the whole evolution of $T_{1\rho}$ as a function of the rf field amplitude can be interpreted in terms of spatial inhomogeneity of the spin-locking rf field (in addition it should lead to a more reliable characterization in terms of cross-link density). This analysis yields consistently the true $T_{1\rho}$ along with another term related also to cross-link density. The other dynamical properties considered in this work, namely transverse relaxation and self-diffusion of a solvent imbedded in the rubber material, are certainly more difficult to deal with, as far as one is essentially interested in cross-link density. The former, because its interpretation is difficult and prone to some ambiguity, the latter because it requires cumbersome sample preparations and also because of less sensitivity to cross-link density.

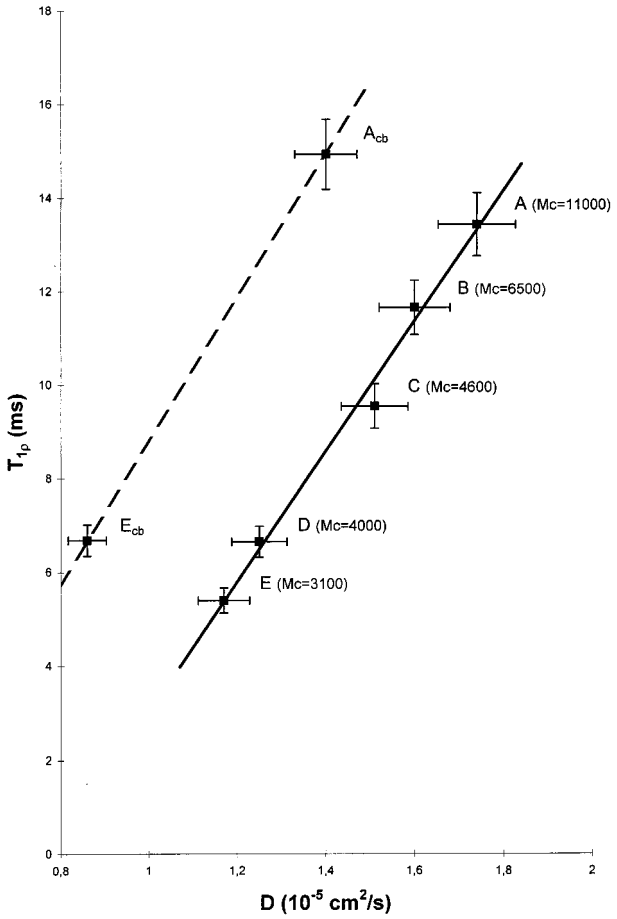

Figure 5. Plots showing the correlation between the self-diffusion coefficient of toluene inside a rubber sample and the proton rotating-frame relaxation time of this sample at $\nu_1 = 80$ kHz (see Figure 3).

Acknowledgment. We would like to gratefully acknowledge the suggestions of a Referee, which contributed to improve the manuscript.

References and Notes

(1) Simon, G.; Schneider, H.; Hausler, K.-G. *Prog. Colloid Polym. Sci.* **1988**, *78*, 31.

(2) Simon, G.; Schneider, H. *Makromol. Chem., Macromol. Symp.* **1991**, *52*, 233.

(3) Brereton, M. G. *Macromolecules* **1990**, *23*, 1119.

(4) Simon, G.; Baumann, K.; Gronski, W. *Macromolecules* **1992**, *25*, 3624.
(5) Cohen-Addad, J. P.; Soyez, E.; Viallat, A.; Queslel, J. P. *Macromolecules* **1992**, *25*, 1259.
(6) Cohen-Addad, J. P. *Prog. NMR Spectrosc*. **1993**, *25*, 1.
(7) Leisen, J.; Breidt, J.; Kelm, J. *Rubber Chem. Technol*. **1998**, *72*, 1.
(8) Fisher, E.; Grinberg, F.; Kimmich, R.; Hafner, S. *J. Chem. Phys*. **1998**, *109*, 846.
(9) Fritzhanns, T.; Demco, D. E.; Hafner, S.; Spiess, H. W. *Mol. Phys*. **1999**, *97*, 931.
(10) Menge, H.; Hotopf, S.; Heuert, U.; Schneider, H. *Polymer* **2000**, *41*, 3019.
(11) *Magnetic Resonance Microscopy*; Blümich, B., Kuhn, W., Eds,; VCH: Weinheim, 1992.
(12) Kuhn, W.; Barth, P.; Hafner, S.; Simon, G.; Schneider, H. *Macromolecules* **1994**, *27*, 5773.
(13) Barth, P.; Hafner, S.; Denner, P. *Macromolecules* **1996**, *29*, 1655.
(14) Spyros, A.; Chrandrakumar, N.; Heidenreich, M.; Kimmich, R. *Macromolecules* **1998**, *31*, 3021.
(15) Schneider, M.; Demco, D. E.; Blümich, B. *J. Magn. Reson*. **1999**, *140*, 432.
(16) Fülber, C.; Demco, D. E.; Weitraub, O.; Blümich, B. *Macromol. Chem. Phys.* **1996**, *197*, 581.
(17) Fülber, C.; Demco, D. E.; Blümich, B. *Solid State NMR* **1996**, *6*, 213.
(18) Sotta, P.; Fülber, C.; Demco, D. E.; Blümich, B.; Spiess, H. W. *Macromolecules* **1996**, *29*, 6222.
(19) Demco, D. E.; Hafner, S.; Fülber, C.; Graf, R.; Spiess, H. W. *J. Chem. Phys*. **1996**, *105*, 11285.
(20) Malveau, C.; Tekely, P.; Canet, D. *Solid State NMR* **1997**, *7*, 271.
(21) Graf, R.; Demco, D. E.; Hafner, S.; Spiess, H. W. *Solid State NMR* **1998**, *12*, 139.
(22) Gasper, N.; Demco, D. E.; Blümich, B. *Solid State NMR* **1999**, *14*, 105.
(23) Schneider, M.; Gasper, L.; Demco, D. E.; Bluemich, B. *J. Chem. Phys.*
(24) Eulry, V.; Tekely, P.; Humbert, F.; Canet, D.; Marcilloux, J. *Polymer* **2000**, *41*, 3405.
(25) Callaghan, P. T.; Samulski, E. T. *Macromolecules* **1997**, *30*, 113.
(26) Kimmich, R. *NMR − Tomography, Diffusometry, Relaxometry*; Springer-Verlag: Berlin, Heidelberg, 1997.
(27) O'Brien, J.; Cashell, E.; Wardell, G. E.; McBrierty, V. J. *Macromolecules* **1976**, *9*, 653.
(28) Kenny, J. C.; McBrierty, V. J.; Rigbi, Z.; Douglass, D. C. *Macromolecules* **1991**, *24*, 436.
(29) Amin, M.; Nasr, G. M.; Attia, G.; Gomaa, A. S. *Mater. Lett*. **1996**, *28*, 207, and references therein.
(30) See for instance: Canet, D. *Nuclear Magnetic Resonance, Concepts and Methods*; Wiley: Chichester, 1996.
(31) Humbert, F.; Valtier, M.; Retournard, A.; Canet, D. *J. Magn. Reson.* **1998**, *134*, 24.
(32) Dybowski, C.; Pembleton, R. G. *J. Chem. Phys.* **1979**, *70*, 1962.
(33) Lindberg, J. J.; Törmälä, P. *Europhys. Conf. Macromol. Phys*. **1981**, *51*, 129.